

The Effect of Attenuation on the Identification of Impact Damage in CFRP Laminates

R. BARTHORPE*, K. WORDEN*, M. T. H. SULTAN[†],
M. EATON[&], R. PULLIN[&] and K. HOLFORD[&]

ABSTRACT

The subject of this study is the identification of impact damage in composite materials on the basis of response-only measurements. Low velocity impact events can lead to barely visible damage in composite structures which if left undetected can lead to degradation of performance and, in the worst case, to catastrophic failure of the structure. The increasing use of composite materials in aerospace and renewable energy applications motivates a desire to develop methods that allow detection of impact and identification of any resulting damage using measured responses only. In previous work it has been shown that low-dimensional ‘features’ drawn from surface mounted sensors may be used to develop a statistical basis for damage identification for Carbon Fibre-Reinforced Polymer (CFRP) coupon samples subjected to impact via a drop-test machine. This work has shown that not only can such features be used to indicate the presence of damage, but also that they show promise in indicating both the nature and extent of the damage that has occurred. There are several questions outstanding with regards to this method of damage identification. Prominent among these is the question of attenuation of the signal as it passes through the structure and whether this will hinder the practical application of the methodology. Attenuation is a particular concern given the nature of the composite materials under investigation, being both moderately damped and orthotropic in nature. In the present study, the effect of attenuation is investigated through a series of experiments on extensive plates with sensors at varying locations and orientations from the point of impact.

^{*}Robert Barthorpe, Keith Worden: Department of Mechanical Engineering, University of Sheffield, Mappin Street, Sheffield S1 3JD, UK., [†]M.T.H Sultan: Department of Aerospace Engineering, Faculty of Engineering, University Putra Malaysia, 43400 Serdang, Selangor Darul Ehsan, Malaysia, [&]Mark Eaton, Rhys Pullin, Karen Holford: Cardiff School of Engineering, Cardiff University, The Parade, Cardiff CF24 3AA, UK.

INTRODUCTION

Recent years have seen a substantial growth in the use of fibre-reinforced polymers in aerospace applications thanks to their superior strength-to-weight attributes and in-service durability. It is, however, well known that composites are far more susceptible to impact damage than metallic alternatives [1]. To complicate matters, such damage is often barely visible on the surface of the material. This motivates the search for technologies that enable in-service monitoring of composite aerospace structures in order that the occurrence and extent of potentially damaging impacts may be identified at an early stage. A method that makes use of only response measurements from PZT sensors was proposed in previous works by the authors [2, 3] and demonstrated for coupon samples. The method allowed both detection and estimation of the extent of damage to be made through analysis of the power spectra of the recorded signals. The methods are based on the finding that higher energy impacts result in a greater proportion of the signal power being focused in the higher frequencies.

The principle aim of the present paper is to investigate the effect of attenuation on the performance of the previously proposed method. It is well-known that wave attenuation through composite materials is far more pronounced than in metallic structures and that this has the potential to make application of the proposed damage identification strategy impractical. Severe attenuation would necessitate a dense sensor network in order to detect damage and this is undesirable for reasons of cost, weight and practicality. In order to investigate the effect of attenuation a series of experiments were conducted using more extensive CFRP plates than those previously investigated. An overview of the methodology is as follows.

1. Instrument a number of extensive and nominally identical CFRP panels with PZT sensors
2. Obtain sensor responses resulting from drop tests conducted on each of the plates in turn. The level of impact energy is increased for each panel.
3. Apply an orthogonal wavelet transformation to the derived sensor responses in order to assess the proportion of signal power in the higher frequencies.
4. Analyse the outputs of Step 3 in order to assess the effect of attenuation (resulting both from distance and ply orientation) on the performance of the method.

EXPERIMENTAL PROCEDURE

The experimental programme was conducted in test facilities at Cardiff University. The CFRP laminate panels were manufactured in-house in the Cardiff autoclave. They comprised eight plies of Cytec woven carbon fibre material in a $0^{\circ}/90^{\circ}$ lay-up. The sensors used were Sonox P5 discs with a diameter of 10mm and thickness of 1mm. Acquisition of PZT data for the present study was conducted alongside the acquisition of data via other sensing hardware (acoustic emission (AE) and macro fibre composite (MFC) sensing). The outcomes of the AE and MFC acquisition are not considered further here.

The location of the sensors is illustrated in Figure 1 and described in Table 1. The sensors were located so as to enable a comparison of attenuation effects arising both from distance and orientation. It is postulated that the attenuation effect will be less pronounced when wave travel is parallel to the ply direction. Acquisition of time-series voltage data was performed using LMS SCADAS equipment. The analysis can be applied directly to the voltages, so no sensitivity calibration was required.

Table 1. Sensor location.

| Sensor | Angle | Distance |
|--------|-------|----------|
| S1 | 0° | S1 |
| S2 | 60° | S2 |
| S3 | 90° | S3 |
| S4 | 150° | S4 |
| S5 | 180° | S5 |
| S6 | 240° | S6 |

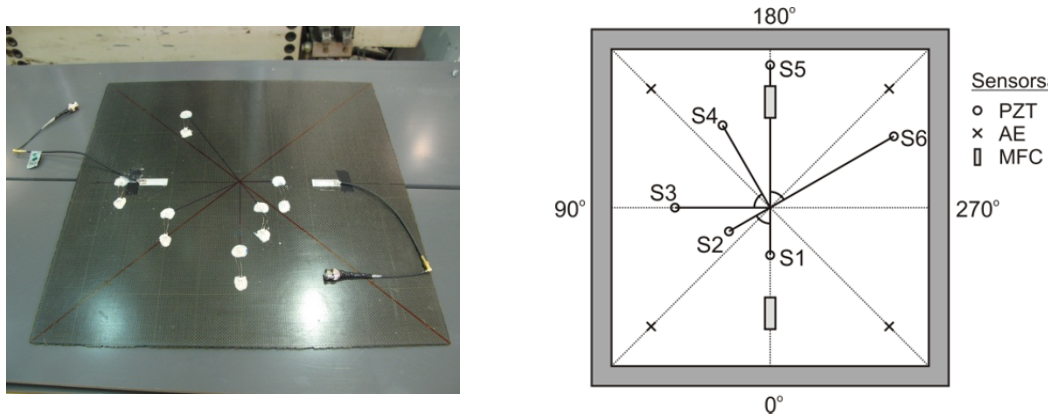


Figure 1. (a) Panel 1 instrumented with six PZT and two MFC patches; (b) schematic of sensor layout.

A total of five nominally identical plates were used for the main test. The plates were mounted between two square frames fabricated from box steel. The frames were clamped to the bed of the drop test rig at each corner. Impacts were applied to the centre of the plate using an Instron Dynatup 9250HV impact test machine instrumented with a 13mm diameter hemispherical head. Trial runs at 8J, 16J and 20J were conducted using a scrap (i.e. previously damaged) plate in order to set an appropriate range for the main test. Damage in this specimen was checked via C-scan after each impact. The final experimental programme is detailed in Table 2. Also shown is whether MFC patches were present for each test.

Table 2. Experimental programme.

| Panel | Energy | MFCs |
|-------|--------|------|
| 1 | 8J | |
| 2 | 12J | ✓ |
| 3 | 16J | ✓ |
| 4 | 20J | |
| 5 | 24J | |

Having conducted the first test it was found that the initial measurement range set for the PZT sensors ($\pm 10V$) was exceeded for several sensor locations. As $\pm 10V$ was the maximum range available for the LMS equipment employed a decision was made to apply voltage attenuators to each of the channels, stepping down the voltage. Unfortunately only four such attenuators were available. These were fitted to sensors S1, S3, S5 and S6 to allow comparison of three distances from impact (60, 120 and 180mm) and on-ply and off-ply behaviour for the 180mm case. Responses from sensors S2 and S4 were still recorded and are included in the analysis below.

WAVELET ANALYSIS

In the first studies of the method [2,3], two independent steps were used to obtain the features that were used to infer whether a given impact had caused damage. The first step involved separating out the high-frequency content of the response time history using the continuous wavelet transform; the second used the frequency centroid of the spectrum as a means of locating how much high-frequency content resulted. In the current study, the discrete wavelet transform will be adopted instead.

The wavelet transform is a linear transformation that decomposes a given function $x(t)$ into a superposition of elementary functions $\psi_{a,b}(t)$ derived from an *analysing* or *mother* wavelet $\psi(t)$ by scaling and translation i.e.,

$$\psi_{a,b}(t) = \psi^* \left(\frac{t-b}{a} \right) \quad (1)$$

where $*$ denotes complex conjugation, b is a translation parameter indicating the time locality and a ($a > 0$) is a dilation or scale parameter. Because of the incorporation of the translation parameter, the wavelet transform - unlike the Fourier transform - is ideally suited to the analysis of nonstationary signals [4]. Given the basis of elementary functions in equation (1), the *continuous wavelet transform* (CWT) is defined as,

$$W_{\psi}^x(a, b) = \frac{1}{\sqrt{a}} \int_{-\infty}^{\infty} x(t) \psi_{a,b}(t) dt \quad (2)$$

The continuous wavelet transform has many useful properties which have been very widely studied (a good reference is [5]); however, if the data of interest are sampled and thus confined to a discrete set, the *discrete wavelet transform* (DWT) can be used with reference to a finite set of translation and dilation parameters. The *dyadic* transform results from setting the dilations and translations to be $a_j = 2^j$ and $b_{j,k} = k/2^j$. Within the dyadic framework, the *orthogonal wavelet transform* (OWT) can be defined. A function $\psi(t)$ is called an orthogonal wavelet if the family,

$$\psi_{m,k}(t) = 2^{\frac{m}{2}} \psi(2^m t - k) \quad (3)$$

(with m and k integers) forms an orthonormal basis of $L^2(\mathbb{R})$, which is to say that,

$$\langle \psi_{m,k}, \psi_{n,l} \rangle = \delta_{mn} \delta_{kl} \quad (4)$$

for all allowed integers m, n, k, l , where $\langle \sim, \sim \rangle$ is the usual inner product defined by,

$$\langle h, g \rangle = \int_{-\infty}^{\infty} h(t)^* g(t) dt \quad (5)$$

and δ_{nm} is the Kronecker symbol which equals unity if $m = n$, and zero otherwise. The orthogonal wavelet transform can now be defined by,

$$x_k^m = \int_{-\infty}^{\infty} x(t) \psi_{m,k}(t) dt \quad (6)$$

The transform is simply a linear combination of the basis functions. The scale decomposition leads to a partitioning in the time-domain that is finer at the higher scales. Any decomposed function can be represented as a sum of m wavelet levels,

$$x_{m(t)} = \sum_k x_k^m \psi_{m,k}(t) \quad (7)$$

These levels represent the time behaviour of the signal within different scale bands and gives their contribution to the total signal energy; higher levels refer to finer scales or higher frequencies.

The inverse transform or synthesis formula for the orthogonal decomposition is,

$$x(t) = \sum_{m,k} x_k^m \psi_{m,k}(t) = \sum_m x_m(t) \quad (8)$$

which simply represents a sum over the levels.

The OWT was computed throughout this work using the C-code provided by [6] and made use of the *Daubechies* family of wavelets [7]. Once the wavelet levels have been extracted, computing their variances gives a coarse but useful indication how the power in the original signal is distributed between a number of frequency bands. Higher variances in the higher levels indicate that more power is present at higher frequencies. The level variances will be used in this paper to show that higher energy impacts results in a higher proportion of the signal power in the higher frequencies.

RESULTS

Because of the adoption of wavelet level variances as features here, the analysis of the signals is simplified. Each response signal is transformed using the OWT and the level variances are obtained. The variances are then normalised by division by the total summed variance; this gives the proportions of power in each frequency band corresponding to a level. Recall that the hypothesis was that higher energy impacts causing more damage would result in a higher proportion of high frequency response. As there were altogether 30 responses (5 panels by 6 sensors) generated by the experiment, only the sensor 1 results will be presented here in any detail. Also, rather than showing all of the level decomposition, it will prove sufficient to only show the structure of the two highest levels (called here detail 1 and detail 2) and a residual sum

over all lower levels (called the approximation here). Figure 2 shows the details and approximation for the panel 1, sensor 1 response (lowest energy) impact.

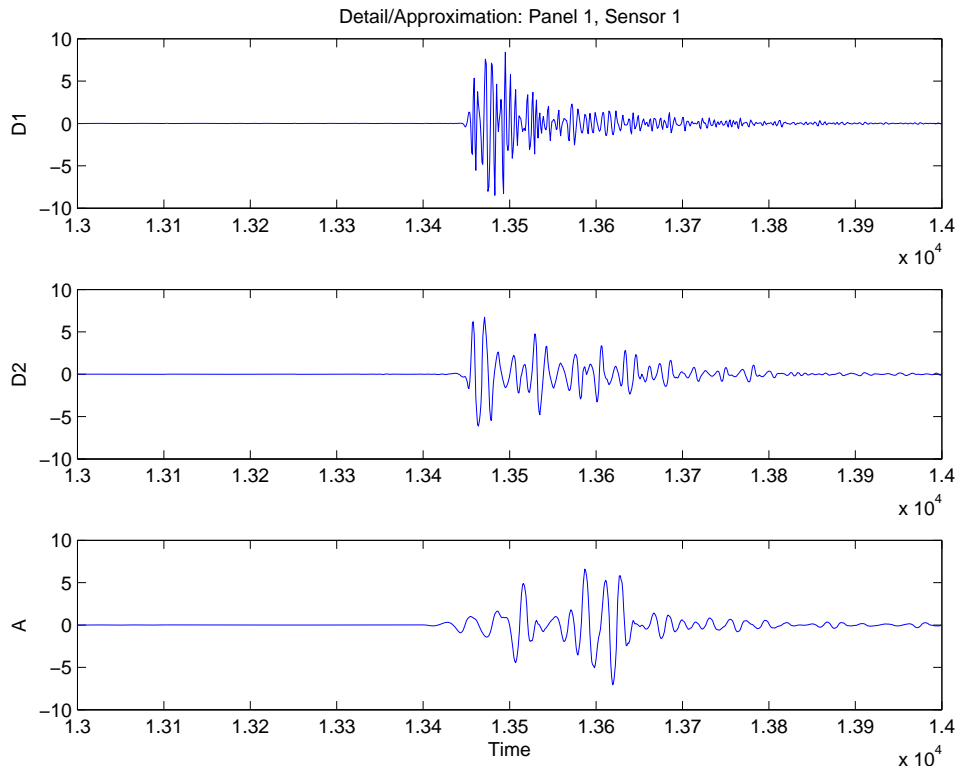


Figure 2. Detail/approximation decomposition for panel 1, sensor 1 impact response.

Figure 2 shows that roughly equal proportions of power are present in the two detail signals and the approximation. There is also an indication that the higher frequency components are arriving earlier, which is consistent with what was observed in [2] and [3]. Figure 3 shows the corresponding decomposition for the panel 5 sensor 1 impact response – i.e. the response associated with the highest energy impact. (Note the vertical scale mismatch between Figures 2 and 3; this is not important as only the relative proportions of amplitudes are important.)

The vertical scales in Figure 3 show that there is a much higher proportion of power in detail 1 (highest frequency) than in the other detail and approximation. In fact, if one considers all five panels in order of impact energy one observes a consistent redistribution of impact response energy into the highest levels. Figure 4 summarises the information by plotting the normalised level variances for each plate from the sensor 1 signals. The figure supports the conclusion that higher energy impacts generate a greater proportion of higher frequency content. As the variances are normalised, it is sufficient to consider the sum of the highest two level variances as an indicator of redistribution of power to higher frequency bands. When one considers this index for the sensor 1 results, one finds that it increases almost monotonically with impact energy. The index is shown in Figure 5 together with all the corresponding indices from the other sensors.

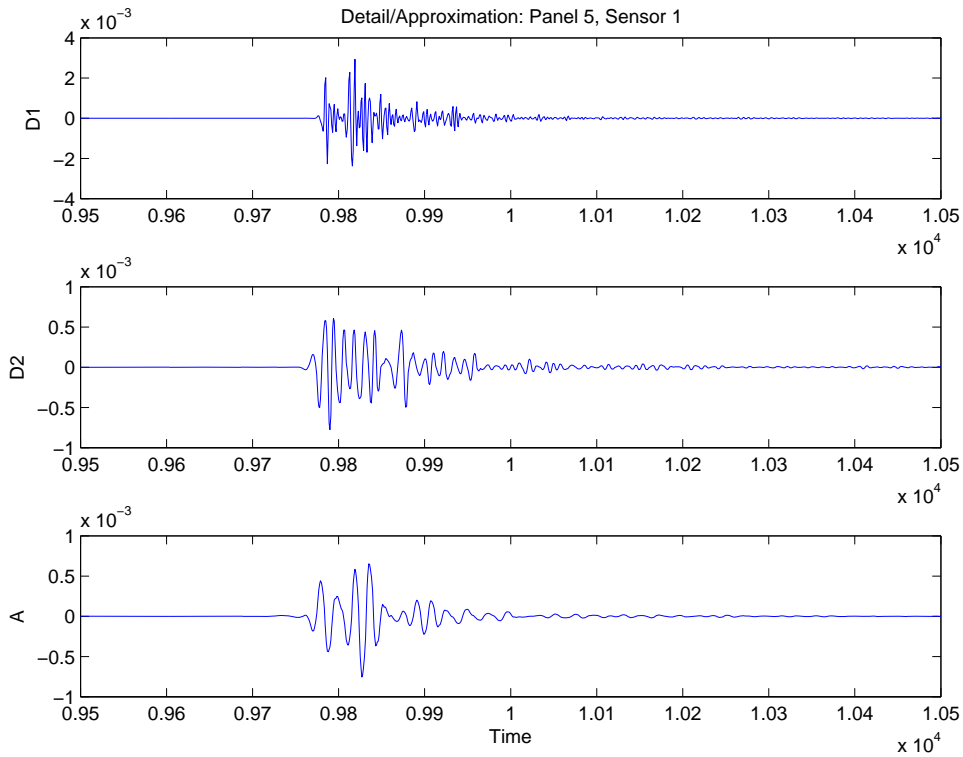


Figure 3. Detail/approximation decomposition for panel 5, sensor 1 impact response.

The first observation is that only the indices from sensors 1 and 2 are monotonic with impact energy; however, the other indices largely increase from panel 1 onwards with isolated fluctuations. The exception to this observation is sensor 6. All the sensors show a marked increase in the index going from panel 1 to panel 2; this is desirable as panel 1 suffered the lowest energy impact and it was thought that this panel may not have been damaged (although it remains to confirm this). For all sensors 1 to 5, the index is lowest for panel 1; however the sensor 6 results are not sensible as a damage indicator because higher energy impacts produce an index lower in value than that for sensor 1. As an overall conclusion, except for sensor 6, the results confirm the idea that higher energy impacts manifest their effect in the response through heightened high frequency content.

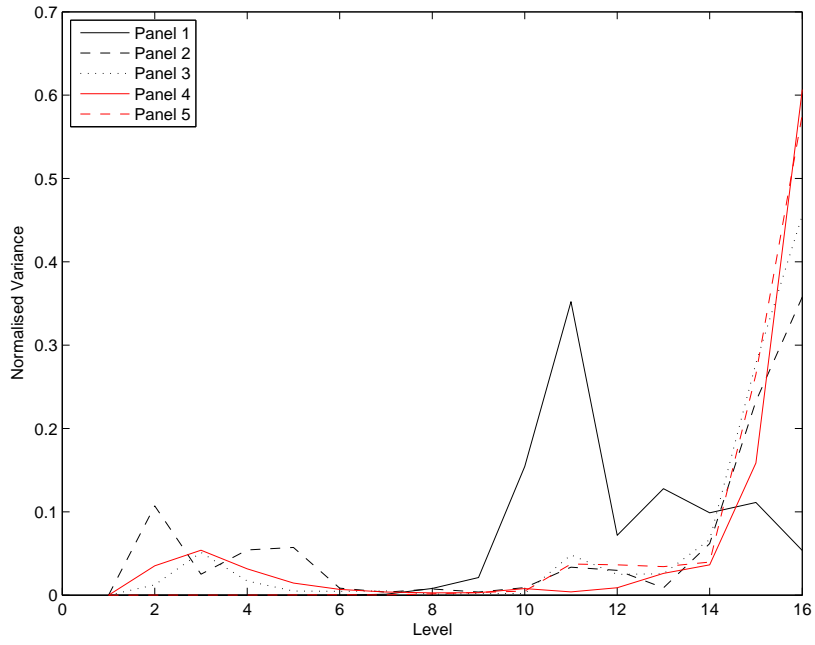


Figure 4. Distribution of power (variance) over wavelet levels for sensor 1 (all plates).

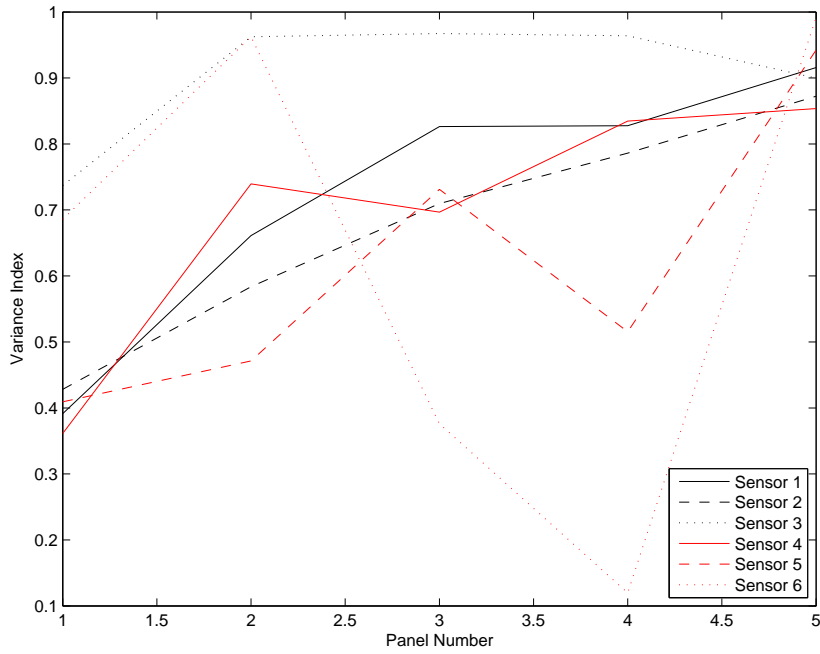


Figure 5. Variance index as a function of panel number (impact energy).

CONCLUSIONS

The results for each sensor are concisely summarised below:

- S1 (on ply, 60mm) and S2 (off ply, 60mm) have performed in a close to ideal manner over the 5 panels, with monotonic increases observed at each damage level.
- S3 (on ply, 120mm) also performed well in the sense that there was an increase in variance between panels 1 and 2. However, having risen to a high level of variance for the panel 2, which was maintained for panels 3 and 4, the index dropped again for panel 5. It could be argued that this sensor was not particularly discriminative.
- S4 (off ply, 120mm) exhibited a small degree of fluctuation for panel 3. Barring this panel, the index increased monotonically with impact.
- S5 (on ply, 180mm) exhibited a slightly greater degree of fluctuation than that seen for S4, most notably for panel 4. Once again, barring this panel, the index increased monotonically with impact.
- S6 (off ply, 180mm) was the location that saw the greatest degree of unexpected fluctuation, particularly for panels 3 and 4.

One conclusion that can be tentatively drawn from the above is that the performance of the applied method did appear to be influenced to an extent by attenuation. This effect manifested itself as a lessening of the *clarity* of the results for the purposes of impact evaluation as opposed to a reduction in their *sensitivity*. It is acknowledged that this study alone is insufficient to draw decisive conclusions on the nature of the attenuation behaviour and that a number of outstanding questions remain. However, the findings are consistent with the hypothesis that attenuation arising both from distance and orientation may have a detrimental effect on impact identification for the method used, even over comparatively small distances. The question of whether this effect will hinder the practical application of the approach remains to be established.

REFERENCES

1. Abrate, S., (1998) *Impact on Composite Structures*. Cambridge University Press.
2. Sultan, M.T.H., Worden, K., Pierce, S.G., Hickey, D., Staszewski, W.J., Dulieu-Barton, J.M. & Hodzic, A., (2011) *On impact damage detection and quantification for CFRP laminates using structural response data only*. Mechanical Systems and Signal Processing 25 pp. 3135–3152.
3. Sultan, M.T.H. Worden, K., Staszewski, W.J. & Hodzic, A., (2012) *Impact damage characterisation of composite laminates using a statistical approach*. Composite Science and Technology, in press.
4. Kaiser, G., (1994) *A Friendly Guide to Wavelets*. Birkhauser.
5. Chui, C.K., (1992) *An Introduction to Wavelets*. Academic Press.
6. Press, W.H., Flannery, B.P., Teukolsky, S.A., & Vetterling, W.T., (1986). *Numerical Recipes - The Art of Scientific Computing*. Cambridge University Press.
7. Daubechies, I., (1992) *Ten Lectures on Wavelets*. SIAM monographs.